Partition of the North Pacific Ocean Based on Similarity in Temporal Variations of the SST Anomaly

By Naoto Iwasaka, Kimio Hanawa and Yoshiaki Toba

Department of Geophysics, Faculty of Science, Tohoku University, Sendai 980, Japan

(Manuscript received 3 August 1987, in revised from 23 April 1988)

Abstract

In order to understand the characteristics of large-scale SST anomaly fluctuations, a cluster analysis with respect to similarities in their temporal variation is made of the SST anomaly field in the North Pacific. This analysis can extract a subdomain of coherent SST anomaly fluctuations in the middle latitude western part of the North Pacific (REGION A), although previous EOF studies of the SST anomaly in the North Pacific did not extract such a subdomain. In addition, the North Pacific Ocean is divided into four major subdomains, that is, the northwestern subdomain (REGION A), the western tropical subdomain (REGION B), the central North Pacific (REGION C), and the eastern boundary region (REGION D). Oceanic and atmospheric conditions characterizing such subdomains are discussed.

1. Introduction

Observed large-scale sea surface temperature (SST) anomaly fluctuations in the North Pacific Ocean have been studied by several authors (*e.g.*, Namias, 1969, 1973, 1978, 1980; Namias and Born, 1970). Although these studies focused only on variations with time scales longer than one month, they have resulted in considerable knowledge of the SST anomaly variations. In particular, studies using the empirical orthogonal function (EOF) analysis revealed dominant spatial and temporal features of the SST anomaly fluctuations in the North Pacific (*e.g.*, Davis, 1976; Iwasaka *et al.*, 1987: henceforth cited as IHT) and in the entire Pacific Ocean (*e.g.*, Weare *et al.*, 1976; Kawamura, 1984). These studies have shown that fluctuations of the SST anomaly over the central and eastern North Pacific represented by the derived first mode of the EOF (EOF 1) (see, *e.g.*, IHT) are closely related to the PNA teleconnection pattern (Wallace and Gutzler, 1981).

While the EOF analysis gave interesting results, the SST anomaly variations in the western North Pacific did not appear for the particular mode of the EOFs in these studies. However, this does not imply that there is no dominant pattern in the SST anomaly fluctuations over the western North Pacific, since the EOF analyses decompose such a pattern into several orthogonal functions. Simultaneous correlation analyses between the time series of the SST anomaly of a particular grid point (reference point) and those of the other grid points suggest that in the middle latitudes of the western North Pacific region, the SST anomaly fluctuates coherently and its characteristics are very different from those in the other regions. That is, as shown in Fig. 1a (see also Fig. 4a of Wallace and Jiang, 1987), the geographical distributions of correlation coefficients (correlation pattern) for the reference points in the central or eastern

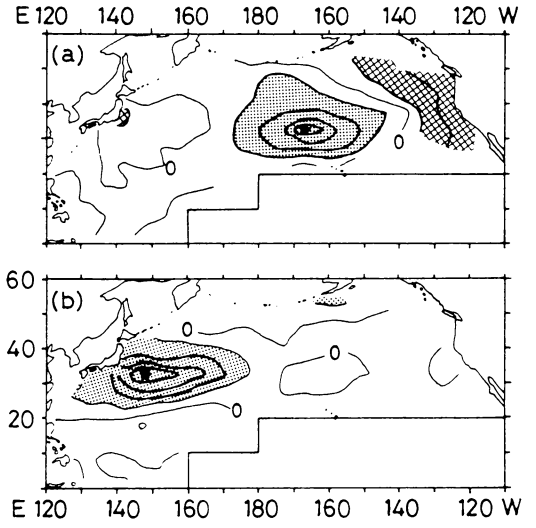

Fig. 1. One-point correlation maps for the reference point of (a) 32.5°N, 167.5°W, and (b) 32.5°N, 147.5°E, respectively. These maps show the spatial distributions of simultaneous correlation coefficients between the SST anomaly time series of the reference point and those of the other points. The dotted area indicates the correlation coefficients which are above 0.2 and cross-hatched area below −0.2. The contour interval is 0.2.

North Pacific resemble the spatial pattern of the EOF 1 obtained by IHT. In addition, it is noted that in the western North Pacific, no significant correlation coefficient appears in Fig. 1a and also no significant amplitude of the EOF 1 exists (Fig. 4 of IHT). On the other hand, it is shown for reference points in the western middle latitudes of the North Pacific that the area where the SST anomaly fluctuates coherently expands from the Japan Islands approximately to the international date line in the middle latitudes and no significant correlation appears in the rest of the region (Fig. 1b).

Therefore, although the EOFs of the SST anomaly in the North Pacific do not conveniently represent such subdomains, it can be expected that the North Pacific Ocean can be divided into several subdomains in which the SST anomaly fluctuates coherently. Further, temporal variations of the SST anomaly in these subdomains are uncorrelated to or out-of-phase with each other. Therefore, to identify such subdomains will give some useful information about the mechanisms governing the large scale SST anomaly fluctuations in each subdomain.

The purpose of the present study is to ascertain the existence of the subdomains where the SST anomaly fluctuates coherently. In other words, it is to partition the North Pacific into several subdomains with respect to similarity in the temporal variations of the SST anomaly. For the purpose of the present study, a cluster analysis method will be employed, since it is known that analysis methods of this type are very useful to classify systematically individual elements of the data set in terms of the "similarity" between the individual elements, or clusters.

The data used in the present study are described in Section 2. In Section 3, a general description of the cluster analysis and its algorithms are presented. The results and brief discussions are given in Section 4.

2. The Data

The data set used in the present study is the monthly means of 5°×5° latitude-longitude grid SST data for the period from 1969 through 1979, which was also used by IHT. This grid-point data set was calculated from the SST data files provided by the Japan Oceanographic Data Center. See IHT for procedures used in the construction of the data set. An anomaly is defined as the residual obtained after subtracting the 11-year mean (1969-1979) monthly mean value from the value for each month. The array of the grid points used are shown in Fig. 2. Only

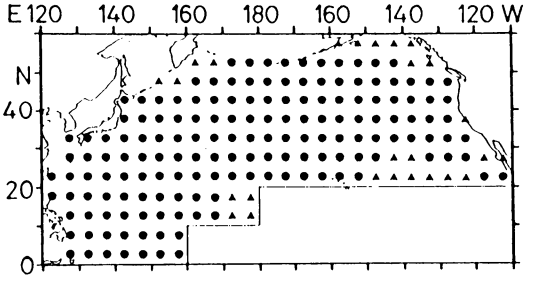

Fig. 2. The array of the 5°×5° latitude-longitude grid for the SST data set. Black circles indicate the grid points on which the data are available for every month in the 11-year (1969-1979) period, and triangles the grid points which have some missing data.

the grid points for which the data are available for every month in the 11-year period, shown as circles (160 points), are selected for the present study. Insufficient data points are shown as triangles.

The monthly mean 500 mb geopotential height data are also used, which were also the same data set as used in IHT.

3. The Analysis Method

Cluster Analysis

Cluster analysis methods have been used to systematically classify individual elements (which are characterized by several properties) of the data set in terms of the "similarity" (or "distance") between the individual elements or clusters (*e.g.*, Anderberg, 1973; Kawaguchi, 1978). These methods have been widely used in the social sciences, psychology, the biological sciences, and others. Recently, since a large memory size has become available in computers, several meteorologists have applied these methods to meteorological fields.

Cluster analysis methods are divided into two categories, *i.e.*, the hierarchical clustering methods and the non-hierarchical methods. In the former category, at the beginning of clustering, each individual element in the data set is considered a cluster. At each step in the clustering, the two clusters whose "distance" is a minimum among all possible pairs of clusters are merged into a new cluster. The virtual shortcoming of these methods is that the calculation cannot be performed for large numbers of elements in the data set since the memory size required becomes larger than the computer's capacity. This type of method was used, for example, in Wolter (1987) who analyzed several meteorological fields in the equatorial Atlantic, the eastern equatorial Pacific, and the Indian Ocean in order to investigate the Southern Oscillation, and in Galliani and Filippini (1985) who studied the climate of a small area in the northern region of Italy. Suzuki and Kawamura (1987) used one of these methods to analyze the characteristics of wind systems in Central Japan.

In the latter category, at the beginning of clustering, several individual elements of the data set are chosen as "seed points" and initial clusters are arbitrarily constructed around these points. At each successive step of the clustering, the average deviation of the individual elements of a cluster from its seed point is calculated, then the seed points are re-chosen and individual elements are redistributed and/or exchanged between clusters. These processes are repeated until the average deviation for each cluster becomes smaller than a given value. When using this method, it is difficult to specify how the number of seed points should be determined. This type of method was used, for example, in Mo and Ghil (1987) who analyzed the 500 mb height field over the Northern Hemisphere. Maryon and Storey (1985) used the result of this type of cluster analysis in a multivariate statistical model used for forecasting.

The Ward Method

In the present study, the Ward method, one of the hierarchical clustering methods, is employed, basically for two reasons:

(1) it is unknown how many subdomains (*i.e.*, clusters) the North Pacific should be divided into, and
(2) the centroid of each cluster obtained by this method can be treated as representative of the cluster.

This method was proposed initially by Ward (1963), and later Wishart (1969) developed a practical algorithm for its calculation. The concept of the Ward method is as follows (Wishart, 1969): let the data set consist of n-elements and each element be characterized by m-properties, in other words, each element of the data set be identified as a point in m-dimensional Euclidean space, such as

$$T_{i,j}: \ i=1 \text{ to } n, \ j=1 \text{ to } m$$

or

$$T_i=T_i(T_{i1}, \cdots, T_{ij}, \cdots, T_{im}) \ ; \ i=1 \text{ to } n.$$

At any stage in this analysis, the "loss of information", E, which results from the grouping of points into a cluster, can be measured by the total sum of the squared deviations (or within-group-error: Anderberg, 1973), E_k, of every point from the mean of the cluster to which it belongs. That is,

$$E=\sum_k E_k,$$

where

$$E_k=\sum_{i=1}^{N_k}\sum_{j=1}^{m}(T_{ij}-TM_j^k)^2, \quad \text{and}$$

$$TM_j^k=\sum_{i=1}^{N_k}T_{ij}/N_k.$$

At each step in the analysis, the union of every possible pair of clusters is considered, and the two clusters whose fusion results in the minimum increase in E are combined. Initially, each of the individual points are regarded as a single-point cluster, and the first fusion clearly involves those two points which are closest. At subsequent steps, however, the fusion of multi-point clusters must be considered.

Algorithm of the Ward Method

The algorithm of the Ward method used in the present study is as follows: let

$T_i(t)$

be the SST anomaly time series for i-th grid point, i=1 to 160, and let

$$E_k=\sum_{i=1}^{N_k}\sum_{t=1}^{N_t}(T_i(t)-TM^k(t))^2/N_k \qquad (1)$$

be the squared deviations for the cluster k, where N_t is the number of months in the time series $T_i(t)$. Also, let

$$TM^k(t)=\sum_{i=1}^{N_k}T_i(t)/N_k$$

be the centroid of cluster k, $i=1$ to N_k, where T_i belongs to the cluster k.

N_k is the number of grid points of the cluster k, and

$$E=\sum_k E_k$$

is the loss of information.

As mentioned above, at each step of clustering in the Ward method, those two clusters whose fusion results in a minimum increase in E should be found. Wishart (1969) showed that the two clusters whose "distance" D_{ij}^2 is minimum among all possible pairs of clusters are identical pair of clusters which results in the minimum increase in E, where

$$D_{ij}^2=((N_i+N_h)D_{ih}^2+(N_i+N_k)D_{ik}^2-N_iD_{hk}^2)/(N_i+N_j). \qquad (2)$$

Here the cluster j is a fusion of clusters h and k, $N_j=N_h+N_k$, and at the first step, D_{ij}^2 is set to be the Euclidean distance between $T_i(t)$ and $T_j(t)$.

Therefore, the algorithm for the Ward method in the present study is,

(a) at initial stage, calculation of the Euclidean distances between T_i and T_j,
(b) searching for the two clusters whose distance is a minimum,
(c) merging those two clusters to create a new cluster, and
(d) recalculating the distances D_{ij}^2 defined by (2) among the new clusters and others, then repeating step b, c, d, etc.

In the present study, the time series for each grid point was normalized by its standard deviation before applying the Ward method, since a similar temporal variation in the SST anomaly would be expected to be caused by identical mechanisms.

Criteria for Determination of the Final Number of Clusters

The cluster analysis method, in general, does not have criteria to determine the final number of clusters in the analysis. In the present study, the criteria are adopted as follows:

(1) to make the number of clusters as small as possible, in other words, to make the resulting subdomains as large as possible, and
(2) to keep the correlation between the area-averaged time seies of a particular cluster and almost all time series within that cluster significant.

The reasons for criterion (1) are that the nonseasonal variations of the SST are not expected to occur randomly in space and that since large scale SST anomaly fluctuations are thought to be closely related to large scale atmospheric circulation anomalies, *e.g.*, teleconnection patterns, the spatial scales of resulting subdomains are expected to be comparable to those of atmospheric teleconnec-

tion patterns.

For criterion (2), the lower limits of the correlation are set to be 0.3 for the 11-year data which includes all seasons (132 months of continuous data), and 0.5 for the particular season data, winter (December through March), and summer (June through September). The limit for the 132-month data corresponds to the 90% significance level if the SST anomaly time series are assumed to be autoregressive processes. The limit for the winter and summer season data corresponds to the 90% significance level for 11 individual data.

4. Results and Discussion

The results of the cluster analysis for the SST anomaly field in the North Pacific are shown in Fig. 3 for the 11-year data including all seasons (cited as A-Clusters), in Fig. 4a for the winter season (December through March; W-Clusters), and in Fig. 4b, for the summer season (June through September; S-Clusters), with respect to the similarity in the temporal variation of the SST anomaly.

The results of A-Clusters in Fig. 3 show that the North Pacific Ocean has been divided into four major subdomains: the northwestern part of the North Pacific (henceforth referred to as REGION A), the western equatorial region (REGION B), the central North Pacific (REGION C), the eastern boundary region (REGION D), and one minor subdomain: the eastern subtropical region (REGION E).

In Fig. 5, the time series of the SST anomaly

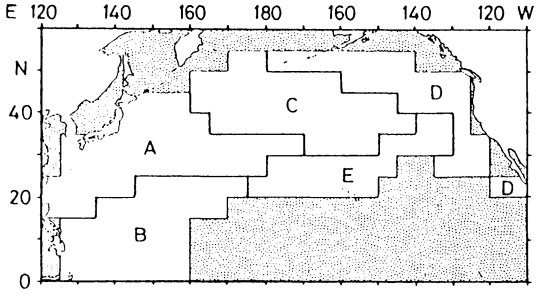

Fig. 3. Results of the cluster analysis for the SST anomaly field for the 11-year (132 continuous months) data including all seasons. Regions labeled A through E indicate the subdomains specified by the five clusters. See the text for the definition of those subdomains.

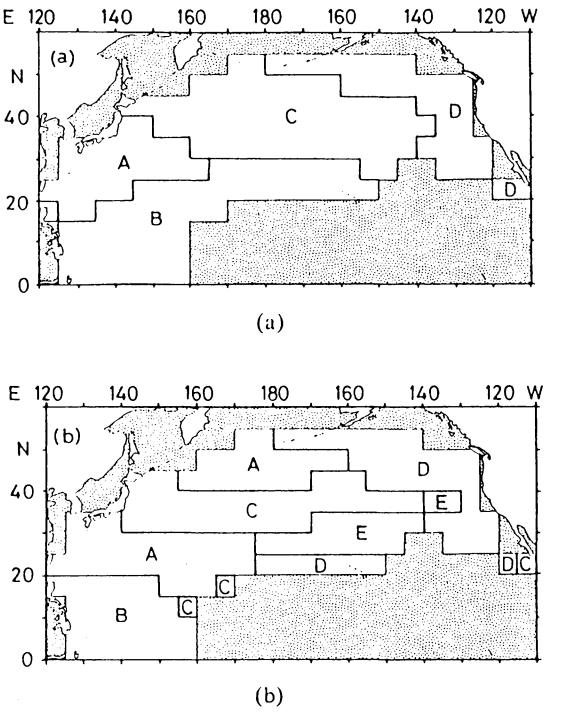

Fig. 4. Same as Fig. 3 except for (a) winter season (December through March), and (b) summer (June through September).

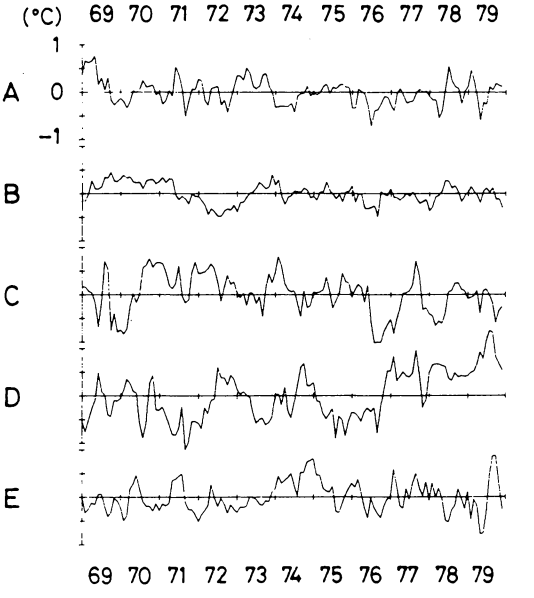

Fig. 5. Time series of the area-averaged SST anomaly for each subdomain shown in Fig. 3.

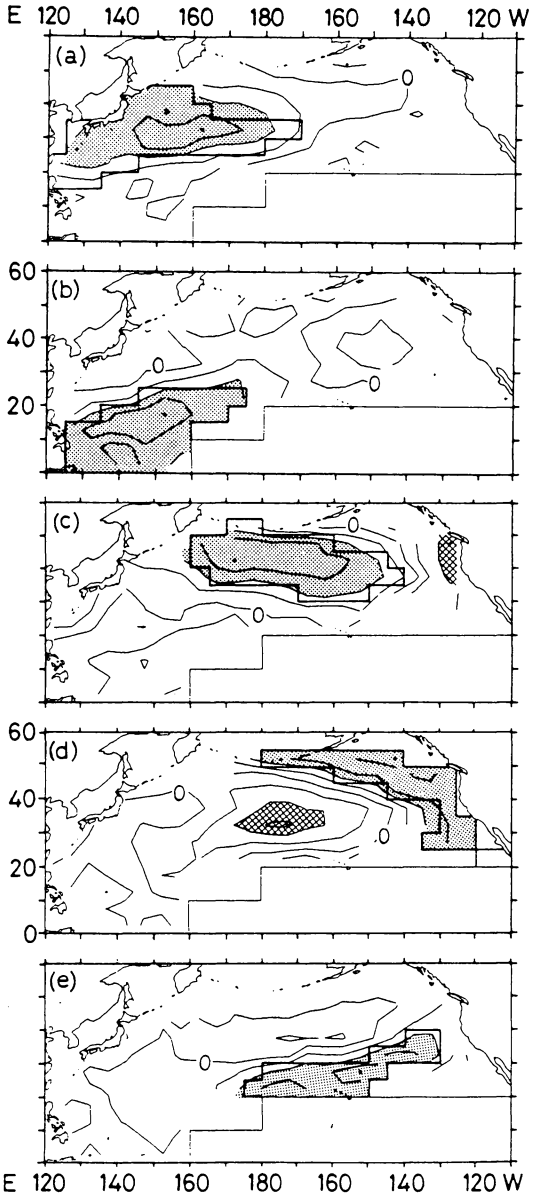

Fig. 6. Geographical distribution of the correlation coefficients among the area-averaged time series of each cluster (subdomain) and those of all grid points of the SST anomaly data set. The dotted area indicates the correlation coefficients which are above 0.4 and cross-hatched area below −0.4. The contour interval is 0.2. Figures (a) through (e) correspond to the time series of REGIONs A to E, respectively. Heavy solid lines denote the borders of each corresponding subdomain.

Table 1. Simultaneous cross correlation coefficients between the time series of the area-averaged SST anomaly for each of the subdomains defined by the cluster analysis and that of the EOF 1 obtained by Iwasaka *et al.* (1987). See the text for the definition of each of these subdomains.

	B	C	D	E	EOF1
REGION A	0.13	0.24	-.17	-.07	0.38
REGION B	.....	0.04	-.08	0.00	0.14
REGION C		.....	-.25	-.01	0.69
REGION D			.....	0.14	-.84
REGION E				.....	-.14

are shown for particular regions of A-Clusters given in Fig. 3. These time series were calculated as the spatial average of the non-normalized local time series over the region specified by the corresponding cluster. Figures 6a to 6e, give the distribution of the simultaneous correlation coefficient between the area-averaged time series of each subdomain of the A-Clusters shown in Fig. 3 and the time series of all grid points are presented for each cluster. Figure 7 shows the distribution of simultaneous correlation coefficients between the time series for A-Clusters shown in Fig. 3 (except for REGION E) and the 500 mb geopotential height anomaly fields. For the time series of REGION E, no significant correlation coefficient appears. Table 1 shows the simultaneous cross correlation coefficient among time series shown in Fig. 5.

Resulting clusters (subdomains) shown in Fig. 3 apparently satisfy criterion (1) mentioned in Section 3. Figures 6a to 6e show that criterion (2) is also satisfied by these clusters.

The results for winter (W-Clusters, Fig. 4a) are similar to those shown in Fig. 3 with the following minor differences: REGION C is expanded both eastward and westward, and REGION E in Fig. 3 is merged into REGION B. This fact confirms that results of the A-Cluster reflect the upper ocean structure as well as the W-Cluster since deep surface mixed layer develops in winter. On the other hand, in the results for summer (S-Clusters, Fig. 4b), REGIONs A, C, and D are quite different, whereas REGION B is similar. The differences may come from the fact that, in summer, the thin seasonal mixed layer that develops within the surface

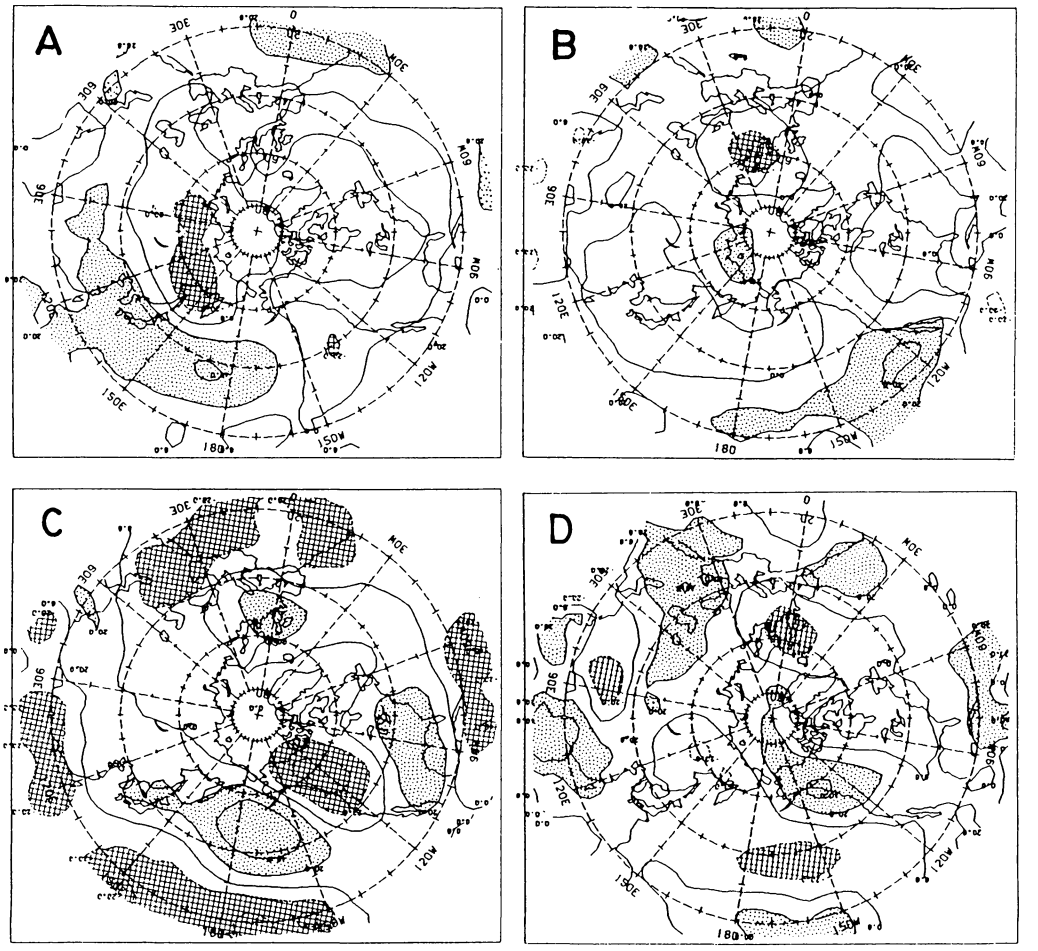

Fig. 7. Geographical distributions of correlation coefficients between the anomalous SST time series averaged within each of the subdomains in Fig. 3 (except for REGION E) and the 500 mb monthly mean geopotential height anomaly. Dotted area indicates the correlation coefficients which are above 0.2 and cross-hatched area below −0.2. The contour interval is 0.2.

layer in middle and high latitudes masks the oceanic subsurface conditions. In the present stage, only this result is presented and interpretation is left for a future work.

In Table 1, the correlation coefficient between REGIONs C and D suggests a weak but out-of-phase relationship, which is expected by the EOF 1 of IHT or the correlation pattern shown in Fig. 1a. REGIONs A and C show a weak positive correlation, which may come from the shape and arrangement of the subdomains in the corresponding regions of S-Clusters (Fig. 4b). It can be noted, however, that the time series of the area-averaged SST anomaly for the subdomains do not correlate significantly with each other.

As was mentioned in the Introduction, the western portion of the North Pacific belongs to the cluster (REGION A) distinguished from those of the central and eastern portions of the North Pacific, with its eastern boundary found between 160°E and the international date line. The boundary between REGIONs A and B is found almost at the same position as that of the Subtropical Front (*e.g.*, Uda and Hasunuma, 1969; White *et al.*, 1978).

With respect to the results in IHT, the shape and the arrangement of REGIONs C and D

resemble the spatial pattern of the EOF 1. The time series associated with the EOF 1 has a large positive correlation with that of REGION C and a negative one with that of REGION D (Table 1).

All the results in the present study imply that the results given in Fig. 3 show a reasonable partitioning with regard to the physical processes which may govern the SST fluctuations. The eastern boundary of REGION B and the southern boundary of REGION E remain uncertain due to the lack of data in the central and eastern equatorial Pacific.

In following subsections, based on the accumulated knowledge, the oceanic and atmospheric conditions along with their relationship to the SST will be briefly discussed for the four major subdomains (REGIONs A through D) shown in Fig 3, or in Fig. 4a.

REGION A

The oceanic conditions in this region are governed largely by the western boundary currents of the subtropical and subarctic gyres, *i.e.*, the Kuroshio, the Kuroshio Extension, and the Oyashio. This region and the Gulf Stream region are the two major areas where the net heat flux from the ocean to the atmosphere exhibits maximum values, especially during the autumn and winter (Hsiung, 1985, 1986). Therefore, it can be expected that the SST, or the upper ocean thermal condition, is controlled by the oceanic heat advection and the air-sea interaction through heat fluxes. This inference is supported by Kurasawa *et al.* (1983), who showed that the air-sea heat fluxes and the heat convergence in the ocean caused by the frequent advections of small patches of warm water balance each other in the upper ocean south of Japan.

Since lower atmospheric conditions during winter in this region are characterized by cold surges of the winter monsoon over east Asia, the SST anomaly fluctuations for the winter season are expected to be related to the east Asian Monsoon. Watanabe and Hanawa (1988) investigated the seasonal mean SST anomaly fields for the western North Pacific and their relationships to the east Asian Monsoon. They performed a correlation analysis between the 3-month mean

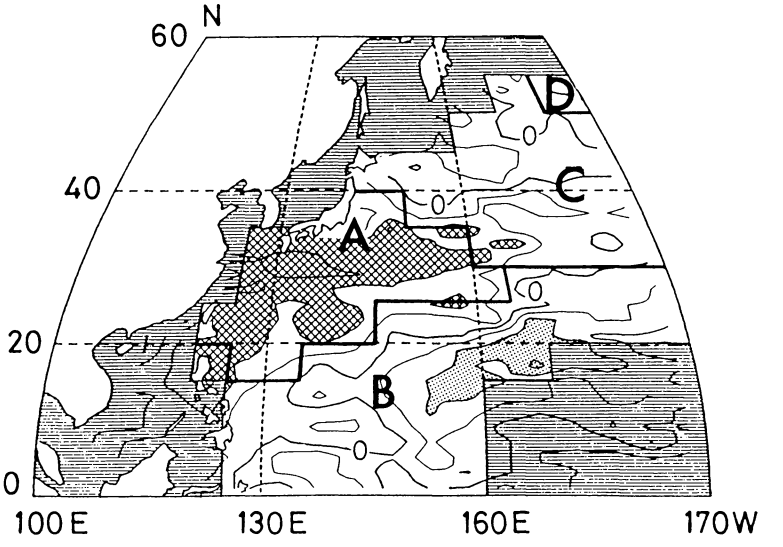

Fig. 8. Geographical distributions of correlation coefficients between the seasonally-averaged SST anomaly and the Monsoon Index (MOI) for the winter season, cited from Watanabe and Hanawa (1988). The dotted area indicates the correlation coefficients which are above 0.4 and cross-hatched area below −0.4. The contour interval is 0.2. Heavy solid lines denote the borders of the REGIONs A to D of W-Clusters. Shaded areas with horizontal lines are the excluded regions in the present study. See the text for definition of the MOI.

2°x5° latitude-longitude averaged SST anomaly and the Monsoon Index (MOI) for the winter season (December through February). The MOI is defined as the amonaly of the sea level pressure difference between Irkutsk (Siberia, USSR) and Nemuro (Hokkaido, Japan). A high MOI corresponds to the winter when cold surges are active. The result of the correlation analysis by Watanabe and Hanawa is shown in Fig. 8, combined with the borders of the REGIONs A through D of W-Clusters. This figure suggests that the anomalous SST in this region during winter is formed by a combination of the amomaly of the oceanic heat convergence and anomalous east Asian Monsoon outbreaks.

Correlation patterns between the area-averaged SST anomaly in this region and 500 mb height field anomaly (Fig. 7a) resembles the WP teleconnection pattern (Wallace and Gutzler, 1981). Kawamura (1984) also obtained the WP pattern from a correlation analysis between the 500 mb height field and the time coefficient of his EOF 2, which represents the SST anomaly fluctuation south of Japan. Nakamura *et al.* (1987) discussed the possibility of an interaction between low frequency variations of the WP pattern, and high frequency baroclinic wave activities in the storm track.

REGION B

The SST in this region exhibits very small temporal variations, including both the climatological mean seasonal variation and the anomaly field. The southern part of this region (south of about 15°N) coincides with the so-called Doldrum region described in Kutsuwada (1988) where the surface wind is very calm. The condition in this region, however, may be closely related to the atmospheric circulation, due to convergence of the surface wind and associated divergence of the wind in the upper-troposphere, which is caused by deep tropical convection. The relationship between the SST and the outgoing long-wave radiation shown by Hirst (1986) indicates that the SST in this region plays an important role in determining atmospheric convective activity, since the SST in practically all of this region is greater than 27°C throughout all seasons.

However, since the 40-60 day oscillation dominates in this region, the one-month mean data used in the present study may not be adequate to analyze the ocean-atmosphere interaction phenomena.

REGION C

As shown in Fig. 3 and Table 1, the shape of this region and the temporal behavior of the SST variations are very similar to those associated with the EOF 1 obtained by IHT. Lag correlation analysis by IHT showed that the SST anomaly fluctuation represented by the EOF 1 may be forced by the PNA teleconnection pattern. Actually, Fig. 7c, which shows the simultaneous relationship between the area-averaged SST anomaly in this region and the 500 mb height anomaly field, also shows a PNA-like pattern. Wallace and Jiang (1987) also showed that correlation coefficients between the SST anomaly at 32°N, 165°W and the 500 mb height field exhibit the PNA pattern. Results of lag correlations between the 500 mb height and the SST anomaly in this region (not shown here) are similar to those between the EOF 1 and the 500 mb height field as shown in IHT.

As noted in IHT, although physical processes of the SST anomaly fluctuation in this region are still not well known, one-dimensional processes, *i.e.*, surface heat flux and/or vertical mixing due to wind forcing, may be the mechanisms responsible. In addition, fluctuations in the current system due to the large scale wind stress curl may cause the variation in the SST field. The SST in this region may force the atmospheric circulation anomaly whose time scale is longer than a season, as discussed, *e.g.*, in Wallace and Jiang (1987). Detailed examinations of this are, however, left for a future study.

REGION D

The SST anomaly variation in this region may also be connected with the PNA pattern, as expected from the results of IHT and Wallace and Jiang (1987). Figure 7d also shows a PNA-like pattern, although it is slightly weaker than that of REGION C.

Besides the one-dimensional processes, and since an eastern boundary exists in this region,

fluctuations of the surface Ekman layer in the ocean caused by an anomalous wind system may be a possible mechanism of the SST anomaly variation. Fluctuations in the current systems along the eastern boundary may also affect the SST anomaly variation. During the period of the El Niño events, long-period sea level anomalies propagating poleward along the eastern boundary have been observed (see, *e.g.*, Chelton and Davis, 1982; Strub *et al.*, 1987). The wave-like disturbances which cause the long-period sea level anomalies may also affect the SST variability in this region, since the long waves influence the volume transport due to the coastal boundary current.

Acknowledgment

The authors are very grateful to Prof. John M. Wallace and Mr. Hisashi Nakamura who kindly read the manuscript and offered many valuable suggestions. They also thank Mr. Tomowo Watanabe for his helpful discussions on the SST anomaly variations in the western North Pacific, and Dr. Atsushi Kubokawa and Dr. Humio Mitsudera for their helpful suggestions.

The present study was performed as part of the Ocean Mixed Layer Experiment, OMLET (Chairman: Y. Toba), one of the Japanese WCRP activities which are financially supported by the Japanese Ministry of Education, Science and Culture.

References

Anderberg, M.R., 1973: *Cluster analysis for applications. Academic Press,* 142-145.

Chelton, D., and R. Davis, 1982: Monthly mean sea-level variability along the west coast of North America. *J. Phys. Oceanogr.*, **12,** 757-784.

Galliani, G., and F. Filippini, 1985: Climatic clusters in a small area. *J. Climatol.*, **5,** 487-501.

Davis, R., 1976: Predictability of sea surface temperature and sea level pressure anomalies over the North Pacific Ocean. *J. Phys. Oceanogr.*, **6,** 249-266.

Hirst, A., 1986: Unstabla and damped equatorial modes in simple coupled ocean-atmosphere models. *J. Atmos. Sci.*, **43,** 606-630.

Hsiung, J., 1985: Estimates of global oceanic meridional heat transport. *J. Phys. Oceanogr.*, **15,** 1405-1413.

———, 1986: Mean surface energy fluxes over the global ocean. *J. Geophys. Res.*, **91,** 585-606.

Iwasaka, N., K. Hanawa, and Y. Toba, 1987: Analysis of SST anomalies in the North Pacific and their relation to 500 mb height anomalies over the Northern Hemisphere during 1969-1979. *J. Meteor. Soc. Japan.*, **65,** 103-114.

Kawaguchi, M., 1978: *An Introduction to Multivariate Analysis II (in Japanese). Morikita-Shuppan,* 26-44.

Kawamura, R., 1984: Relation between atmospheric circulation and dominant sea surface temperature anomaly patterns in the North Pacific during the Northern winter. *J. Meteor. Soc. Japan,* **62,** 910-916.

Kurasawa, Y., K. Hanawa, and Y. Toba, 1983: Heat balance of the surface layer of the sea at Ocean Weather Station T. *J. Oceanogr. Soc. Japan,* **39,** 192-202.

Kutsuwada, K., 1988: Interannual variability of wind stress over the Western North Pacific: spatial characteristics. *J. Climate Appl. Meteor.* (in press).

Maryon, R., and A. Storey, 1985: A multivariate statistical model for forecasting anomalies of half-monthly mean surface pressure. *J. Climatol.*, **5,** 561-578.

Mo, K., and M. Ghil, 1987: Cluster analysis of multiple planetary flow regimes. *J. Geophys. Res.*, (submitted).

Nakamura, H., M. Tanaka, and J. Wallace, 1987: Horizontal structure and energetics of Northern Hemisphere wintertime teleconnection patterns. *J. Atmos. Sci.*, **44,** 3377-3391.

Namias, J., 1969: Seasonal interactions between the North Pacific Ocean and the atmosphere during the 1960's. *Mon. Wea. Rev.*, **97,** 173-192.

———, 1973: Thermal communication between the sea surface and the lower troposphere. *J. Phys. Oceanogr.*, **3,** 373-378.

———, 1978: Multiple causes of the North American abnormal winter 1976-77. *Mon. Wea. Rev.*, **106,** 279-295.

———, 1980: Causes of some extreme Northern Hemisphere climatic anomalies from summer 1978 through the subsequent winter. *Mon. Wea. Rev.*, **108,** 1333-1346.

———, and R. Born, 1970: Temporal coherence in North Pacific sea-surface temperature patterns. *J. Geophys. Res.*, **75,** 5952-5955.

Strub, P., J. Allen, A. Huyer, R. Smith, and R. Beardsley, 1987: Seasonal cycles of currents, temperatures, winds, and sea level over the Northeast Pacific continental shelf: 35°N to 48°N. *J. Geophys. Res.*, **92,** 1507-1526.

Suzuki, R., and T. Kawamura, 1987: Characteristics of the wind systems under typical summer conditions in the Central Japan (in Japanese). *Tenki,* **34,** 715-722.

Uda, M., and K. Hasunuma, 1969: The eastward subtropical countercurrent in the western North Pacific Ocean. *J. Oceanogr. Soc. Japan,* **25,** 201-210.

Wallace, J., and D. Gutzler, 1981: Teleconnections in the geopotential height field during the Northern Hemisphere winter. *Mon. Wea. Rev.*, **109,** 784-812.

Wallace, J., and Q. Jiang, 1987: On the observed

structure of the interannual variability of the atmosphere/ocean climate system. *Proceedings of conference on the variability of the atmosphere and oceans on time scale of a month to several years. Roy. Meteorol. Soc.*, (in press).

Ward, J., 1963: Hierarchical grouping to optimise an objective function. *J. Amer. Statist. Assoc.*, **58,** 236-244.

Watanabe, T., and K. Hanawa, 1988: Relationship between SST of the western North Pacific and Monsoon and Southern Oscillation indices. To be submitted *Ocean Air Int.*

Weare, B., A. Navato, and R. Newell, 1976: Empirical orthogonal analysis of Pacific surface temperatures. *J. Phys. Oceanogr.*, **6,** 671-678.

White, W., K. Hasunuma, and H. Solomon, 1978: Large-scale seasonal and secular variability of the Subtropical Front in the Western North Pacific from 1954 to 1974. *J. Geophys. Res.*, **83,** 4531-4544.

Wishart, D., 1969: An algorithm for hierarchical classifications. *Biometrics*, **25,** 165-170.

Wolter, K., 1987: The Southern Oscillation in surface circulation and climate over the Tropical Atlantic, Eastern Pacific, and Indian Ocean as captured by cluster analysis. *J. Climate. Appl. Meteor.*, **26,** 540-558.

表面水温アノマリの時間変動の類似性にもとづく北太平洋の海域区分

岩坂　直人・花輪　公雄・鳥羽　良明

（東北大学理学部地球物理学教室）

大規模スケールの表面水温アノマリ変動の特徴を理解するために，表面水温アノマリの時間変動の類似性に着目してのクラスター解析を，北太平洋の表面水温アノマリ場に対して行った。この解析によって，表面水温アノマリがコヒーレントに変動する海域として北太平洋の中緯度西部海域がひとまわりの海域（REGION A）として抽出できた。この海域は，北太平洋表面水温アノマリ場の主成分解析では表現できなかったものである。さらに，北太平洋は，四つの主な海域に分けることが出来る。すなわち，北西海域（REGION A），西部熱帯海域（REGION B），北太平洋中央海域（REGION C），東部境界海域（REGION D）である。これらの海域を特徴づける海洋および大気の条件についても議論する。